Carcinogenesis vol.13 no.7 pp.1143–1153, 1992

Comparison of the biotransformation of 1,3-butadiene and its metabolite, butadiene monoepoxide, by hepatic and pulmonary tissues from humans, rats and mice

György A.Csanády[1], F.Peter Guengerich[2] and James A.Bond[3]

Chemical Industry Institute of Toxicology, PO Box 12137, Research Triangle Park, NC 27709 and [2]Department of Biochemistry and Center in Molecular Toxicology, School of Medicine, Vanderbilt University, Nashville, TN 37232, USA

[1]Present address: GSF-Institut für Toxicologie, Ingolstädter Landstrasse 1, D-8042 Neuherberg, Germany
[3]To whom correspondence should be addressed

1,3-Butadiene (BD), a widely used monomer in the production of synthetic rubber and other resins, is one of the 189 hazardous air pollutants identified in the 1990 Clean Air Act Amendments. BD induces tumors at multiple organ sites in B6C3F1 mice and Sprague–Dawley rats; mice are much more susceptible to the carcinogenic action of BD than are rats. Previous *in vivo* studies have indicated higher circulating blood levels of butadiene monoepoxide (BMO), a potential carcinogenic metabolite of BD, in mice compared to rats, suggesting that species differences in the metabolism of BD may be responsible for the observed differences in carcinogenic susceptibility. The metabolic fate of BD in humans is unknown. The objective of these studies was to quantitate *in vitro* species differences in the oxidation of BD and BMO by cytochrome P450-dependent monooxygenases and the inactivation of BMO by epoxide hydrolases and glutathione S-transferases using microsomal and cytosolic preparations of livers and lungs obtained from Sprague–Dawley rats, B6C3F1 mice and humans. Maximum rates for BD oxidation (V_{max}) were highest for mouse liver microsomes (2.6 nmol/mg protein/min) compared to humans (1.2) and rats (0.6). The V_{max} for BD oxidation by mouse lung microsomes was similar to that of mouse liver but >10-fold higher than the V_{max} for the reaction in human or rat lung microsomes. Correlation analysis revealed that P450 2E1 is the major P450 enzyme responsible for oxidation of BD to BMO. Only mouse liver microsomes displayed quantifiable rates for metabolism of BMO to butadiene diepoxide (V_{max} = 0.2 nmol/mg protein/min), a known rodent carcinogen. Human liver microsomes displayed the highest rate of BMO hydrolysis by epoxide hydrolases. The V_{max} in human liver microsomes ranged from 9 to 58 nmol/mg protein/min and was at least 2-fold higher than the V_{max} observed in mouse and rat liver microsomes. The V_{max} for glutathione S-transferase-catalyzed conjugation of BMO with glutathione was highest for mouse liver cytosol (500 nmol/mg protein/min) compared to human (45) or rat (241) liver cytosol. In general, the K_Ms for the detoxication reactions were 1000-fold higher than the K_Ms for the oxidation reaction. Because of the low solubility of the BD and the relatively high K_M for oxidation, it is likely that the V_{max}/K_M ratio will be important for BD and BMO metabolism *in vivo*. *In vivo* clearance constants were calculated from *in vitro* data for BD oxidation and BMO oxidation, hydrolysis and GSH conjugation. The overall activation/detoxication ratio was markedly different for mice (72), rats (5.8) and humans (5.9) and suggest that at concentrations below the K_M for the reactions, mice have a significantly higher ratio of activation/detoxication than do either rats or humans. The differences in the activation/detoxication ratios between mice and rats correlate with the higher carcinogenic sensitivity of mice than rats to BD.

Introduction

1,3-Butadiene (BD*), a widely used monomer in the production of synthetic rubber and other resins, exhibits low acute inhalation toxicity in rodents—LC_{50} > 120 000 p.p.m. (1)—and causes sensory irritation in humans at concentrations of 2000–8000 p.p.m. (2). Occupational exposures to BD can result during production, storage and transport of the chemical. BD has been detected in cigarette smoke (3) and automobile exhaust (4) and is currently listed as one of the 189 hazardous air pollutants in the 1990 Clean Air Act Amendments (5).

BD displays mutagenic activity in *Salmonella typhimurium* but only in the presence of hepatic 9000 *g* supernatant (6–8), indicating that BD is not mutagenic but that its metabolites, possibly butadiene diepoxide (BDE) and/or 1,2-epoxybut-3-ene (butadiene monoepoxide; BMO), are responsible for the observed bacterial mutagenicity. BD is also genotoxic *in vivo*, inducing chromosome aberrations and sister chromatid exchanges in bone marrow cells and micronucleus formation in peripheral blood of male B6C3F1 mice (9,10), but not in Sprague–Dawley rats (10).

BD induces tumors at multiple organ sites in B6C3F1 mice and Sprague–Dawley rats (11–13). In mice, several tissues are targets for BD carcinogenicity, including heart, lung, mammary gland, ovary, forestomach, bone marrow and liver. An activated K-*ras* gene was observed in lung and liver tumors and lymphomas of B6C3F1 mice exposed to BD (14). The striking aspect of BD-induced carcinogenicity is the extreme sensitivity of mice to BD. Tumors were observed in mice at concentrations as low as 6 p.p.m. and steep concentration–response curves were evident for several tumors. The tumor sites in rats are quite different and include the thyroid, mammary gland, Zymbal gland, uterus, testis and pancreas. Rats exhibit a relatively low sensitivity to BD, since tumors occur at BD concentrations (1000–8000 p.p.m.) nearly three orders of magnitude higher than in mice.

The *in vivo* disposition and metabolism of BD has been reported in B6C3F1 mice (15,16), Sprague–Dawley rats (15–17) and in the non-human primate *Macaca fascicularis* (18). BMO is an exhaled metabolite in all three species exposed to BD (16,18,19). The data from these studies indicate that there are significant species differences in the toxicokinetics of BD and BMO. For example, mice have higher circulating blood levels of epoxides compared to rats or monkeys following exposure to BD. *In vitro* studies using lung and liver microsomes of mice, rats and humans (one sample) suggest that mice metabolize BD at significantly greater rates than other species (20,21). The limited human data and the fact that much of the data reported

*Abbreviations: BD, 1,3-butadiene; BDE, butadiene diepoxide; BMO, butadiene monoepoxide; TCPO, 1,1,1-trichloropropene oxide.

for mouse metabolism are in the NMRI strain for which there is no carcinogenicity data limit the usefulness of the existing *in vitro* work for extrapolation to *in vivo* situations.

Three enzymes appear to play major roles in the overall metabolism of BD: cytochrome P450-dependent monooxygenases, epoxide hydrolases and glutathione S-transferases. In addition to enzymic reactions, BD epoxides may non-enzymatically hydrolyze or conjugate with glutathione (GSH). Presently, there are insufficient data that quantitatively describe the contribution of these various pathways in Sprague–Dawley rats and B6C3F1 mice, species susceptible to BD-induced carcinogenesis, or humans, a species potentially at risk for BD. Since one or more of the BD epoxides may play a role in the carcinogenicity of BD, a quantitative understanding of the balance of activation (i.e. epoxide formation) and inactivation (i.e. epoxide hydrolysis or conjugation) is essential for improving our understanding and assessment of human risk following exposure to BD.

The present paper reports quantitative species differences in the oxidation of BD and BMO by cytochrome P450-dependent monooxygenases and in the inactivation of BMO by epoxide hydrolases and glutathione S-transferases using microsomal and cytosolic preparations of livers and lungs obtained from Sprague–Dawley rats, B6C3F1 mice and humans. Our results demonstrate that there are significant quantitative species differences in the activation and inactivation of BD and its epoxide metabolites. The data from these studies provide a quantitative basis for our understanding of the relative contributions of the various pathways of BD metabolism in three animal species, including humans.

Materials and methods

Chemicals

The following chemicals were used: BD (99+% purity) and BMO (98%; Aldrich Chemical Company, Inc., Milwaukee, WI); BD-d_6 (98% enriched; Cambridge Isotopes Ltd, Cambridge, MA), trifluoroacetic acid (97%) (Fischer Scientific, King of Prussia, PA); protein kit based on the modified micro-Lowry method, NADPH (grade III), ethylenediaminetetraacetic acid (99%), GSSG (grade III) and indomethacin (Sigma Chemical Co, St Louis, MO); reduced L-glutathione (Fluka Chemical Co., Ronkonkoma, NY); [glycine-2-^{3}H]glutathione (NEN® Research Products, Du Pont, Boston, MA). Chlorzoxazone, 6-hydroxychlorzoxazone and 5-fluorobenzoxazilinone, an internal standard for the chlorzoxazone 6-hydroxylation assays, were synthesized by R.Peter (University of Erlangen, Germany). 1,1,1-Trichloropropene oxide (TCPO) was a gift from Dr Pat Sabourin (Inhalation Toxicology Research Institute, Albuquerque, NM). All solvents were HPLC grade and all other chemicals were of the highest quality commercially available.

Animals

Male Sprague–Dawley (CD®) rats (9–10 weeks) and male B6C3F1 mice (9–10) weeks were obtained from Charles River Laboratories (Raleigh, NC). Animals were determined to be free from viral infection and were acclimated for at least 2 weeks prior to use. Animals were fed with standard diet (NIH-07; Zeigler Brothers, Gardners, PA) and received water *ad libitum*. All animals were maintained on a 12 h light/dark cycle beginning at 07.00 h and housed at 22 ± 2°C and 55 ± 5% relative humidity.

Preparation of rodent and human liver and lung microsomes and cytosol

Rodents were anesthetized with carbon dioxide. The animals were perfused *in situ* with cold isotonic 0.15 M HCl–0.05 M Tris buffer (pH 7.4). Livers and lungs were weighed, cut into pieces and homogenized with 4 vol of isotonic KCl–Tris buffer with six passes of a Teflon–glass homogenizer (1100 r.p.m., Braun). Homogenates were centrifuged at 10 000 *g* for 20 min at 4°C. After removing the lipid layer, the supernatant was centrifuged at 105 000 *g* for 60 min at 4°C. The supernatant (cytosolic fraction) was stored at −80°C and pellets (microsomal fraction) were resuspended in a wash buffer [0.05 M Tris, 0.25 M sucrose and 1 mM EDTA (22)] with three passes of a Teflon–glass homogenizer (Braun, 1100 r.p.m.). The pellets were collected after a final centrifugation at 105 000 *g* for 60 min at 4°C and rehomogenized in 0.1 M potassium phosphate buffer containing 0.25 M sucrose (pH 7.4) with three passes of a glass–glass homogenizer. Microsomes were stored at −80°C and there did not appear to be any species-dependent effects in storage of microsomes or cytosols Enzyme activities were stable for up to 6 months storage at −80°C.

Samples of liver (n = 12) from trauma victims (Tennessee Donor Services, Nashville, TN) and samples of lung (n = 5) removed by surgery from cancer patients (Cooperative Human Tissue Network, National Cancer Institute, Southwestern Division, University of Alabama at Birmingham, Tissue Procurement Service) were used in these experiments. Due to the small sample size, it was necessary to pool three of the five lung samples for the metabolism experiments. Samples were frozen (−80°C) and remained frozen during shipment. Tissues were slowly thawed on ice, homogenized and microsomes and cytosol were isolated as described above for the rodent tissues. For the human liver samples, typically all 12 samples were used for the initial assessment of reaction rates for an enzyme-catalyzed reaction. The 12 samples were then rank-ordered by enzyme activity and the three samples representing the highest, lowest and median enzyme activities were used for the enzyme kinetic experiments. For determination of BD oxidation kinetics, all 12 liver samples were used.

Protein content was determined using a modified micro-Lowry method (23). Cytochrome P450 content was estimated spectrally as described by Omura and Sato (24).

Cytochrome P450-dependent metabolism of BD and BMO

Microsomes were diluted with 0.1 M phosphate buffer (pH 7.4) to the desired protein concentration. One milliliter of diluted microsomes was placed in each 10 ml vial (Hypo Vial™, Pierce Chemical Co., Rockford, IL) which was sealed with Tuf-Bond™ septa (Pierce Chemical Co., Rockford, IL). Vials were shaken at 37°C in a Dubnoff metabolic shaking incubator. After a 10 min pre-equilibration period, BD (600–25 000 p.p.m.) or BMO (20–200 p.p.m.) in a gas-tight syringe (Hamilton Co., Reno, NV) was injected into the sealed, air-tight vials. After an additional 10 min preincubation the enzymic reaction was started by adding 100 μl NADPH (4 μmol). Preliminary experiments indicated that this preincubation period was essential for equilibration of BD between the liquid and gas phases. The 10 min preincubation did not appear to result in loss of enzyme activity for any of the lung or liver microsomes from any of the species. Preliminary experiments indicated that microsomes were stable for up to 2 h of incubation. Experiments in which BMO was the substrate for the reaction were conducted without the 10 min preincubation.

Air samples (100 μl) were withdrawn from the head-space (i.e. gas-phase) of the vial at 5 min intervals (up to 45 min) and analyzed by GC with a Hewlett-Packard gas chromatograph (HP 5890A Series II) equipped with a flame ionization detector and a 7′ × 1/8″ stainless-steel column filled with Tenax 35-60 mesh. The carrier gas was helium (18.5 ml/min) and the detector, column and injector temperatures were 250, 130 and 200°C respectively. Under these conditions the retention times of BD and BMO were 0.80 and 2.20 min respectively. Calibration curves of BD and BMO were linear in the concentration ranges of 10–55 000 p.p.m. and 1–340 p.p.m. respectively.

Cytochrome P450-dependent metabolism of BMO to BDE was examined using TCPO (1.1 μM) to inhibit the enzymic hydrolysis of BMO by epoxide hydrolase. In some reactions, NADPH was omitted. Liver microsomes were also incubated with chlorzoxazone, a specific substrate for human liver cytochrome P450 2E1 (25,26). The hydroxylation of chlorzoxazone to 6-hydroxychlorzoxazone was measured as previously described (26).

Enzyme-mediated hydrolysis of BMO

Enzyme-mediated hydrolysis of BMO by epoxide hydrolase was measured for the cytochrome P450-dependent reactions except that BMO was used as the substrate for the reaction and NADPH was not added. NADPH was omitted from the reactions to prevent enzymic oxidation of BMO. In some experiments, TCPO (0.25–3.6 μM) was added to inhibit BMO hydrolysis. Both microsomal and cytosolic protein were used in these experiments. To assess the non-enzymic hydrolysis of BMO, reactions were carried out in the presence of heat-inactivated tissue.

Enzyme-mediated conjugation of BMO with GSH

The reaction mixtures (0.1 ml) containing different BMO concentrations (2.5, 7.4, 17.4, 37.1 and 74.5 mM), cytosolic or microsomal protein (1.0 mg/ml) and GSH (10 mM) were placed in Screw Cap Septum vials (Pierce Chemical Co., Rockford, IL) and sealed with Tuf-Bond™ septa. [^{3}H]GSH (40 μCi) was added to the vials and after a 10 min incubation at 37°C, 0.1 ml cooled methanol was added and the precipitated proteins were centrifuged for 1 min at 12 500 *g*. Reactions were linear with time for at least 10 min. An aliquot of supernatant (10 μl) was chromatographed by HPLC (Waters 510 pumps, Milford, MA). Metabolites were separated on a 5 μm C_{18} Ultrasphere column (250 × 4.6 i.d. mm; Beckman) and the absorbance of the effluent was monitored by UV detection (Waters 486 Tunable Absorbance Detector, λ = 263 nm). Metabolites were quantitated by monitoring the radioactivity of the eluant with a Packard FlowOne® Beta inline radioflow detector (Packard, Downers Grove, IL). Analysis was performed under isocratic conditions of methanol/0.1% trifluoroacetic acid (15:85)

with a 1.0 ml/min flow rate. The retention times for GSH, GSSG and the two major GSH conjugates, *S*-(1-hydroxy-3-buten-2-yl)glutathione and *S*-(2-hydroxy-3-buten-1-yl)glutathione, were 3.8, 4.5, 7.8 and 8.5 min respectively. Data on rates of formation of GSH conjugates that are reported represent the sum of the individual rates of formation for each of the conjugates. Recovery of GSH, GSSG and metabolites from the column was >99%. Indomethacin (100 μM), an inhibitor of rat liver glutathione S-transferase (4−4) (27,28), was used to inhibit the enzymic conjugation of BMO with GSH.

Enzyme-mediated conjugation of BMO with GSH was not detected using liver or lung microsomes from humans and mice, and therefore second-order rate constants were determined by incubating microsomes with 100 mM BMO and 10 mM GSH. The initial rates of conjugate formation for the 12 human liver samples ranged between 14 and 98 nmol/min/mg protein. The two samples with the highest and lowest activity were used to determine the second-order rate constants.

Mass spectrometry

A Varian 3500 gas chromatograph with a BD-Wax fused silica column (25 m × 0.3 mm o.d., 0.5 μm film thickness; J&W Scientific, Folsom, CA) was coupled directly to the ion source of a Finnigan 4500 mass spectrometer (San Jose, CA). The oven temperature was maintained at 35°C for 0.2 min and then increased to 150°C (40°C/min) and maintained for 15 min. The carrier gas was helium (2 ml/min) and the mass spectrometer was used in electron-impact mode.

Model development

A two-compartment model was developed to describe the distribution and reaction of BD and BMO in the reaction vials (Figure 1; ref. 21) and to calculate the rate constants for oxidation, hydrolysis, conjugation and distribution. In the model, BD is distributed between the gas phase and the liquid phase containing the reaction mixture. The BD concentration in the gas phase is measured by GC as described above. In the liquid microsomal phase, BD can be oxidized to BMO, which may hydrolyze spontaneously or by the action of epoxide hydrolases, or conjugate with GSH (if present in the reaction mixture). BMO can be further oxidized to BDE, competing with BD for oxidation by cytochrome P450 monooxygenases. BMO also distributes between the liquid phase and gas phase, thereby allowing analysis of BMO in the gas phase by GC. The model equations are:

BD in the gas phase

$$V_g \frac{dC_g^{BD}}{dt} = - V_g k_{12}^{BD} C_g^{BD} + V_l k_{21}^{BD} C_l^{BD} \quad (1)$$

BD in the liquid phase

$$V_l \frac{dC_l^{BD}}{dt} = V_g k_{12}^{BD} C_g^{BD} - V_l k_{21}^{BD} C_l^{BD} - \frac{V_{max}^{Cyt_1} M_{prot} C_l^{BD}}{K_M^{Cyt_1}(1 + C_l^{BMO}/K_M^{Cyt_2}) + C_l^{BD}} \quad (2)$$

BMO in the gas phase

$$V_g \frac{dC_g^{BMO}}{dt} = - V_g k_{12}^{BMO} C_g^{BMO} + V_l k_{21}^{BMO} C_l^{BMO} \quad (3)$$

BMO in the liquid phase

$$V_l \frac{dC_l^{BMO}}{dt} = V_g k_{12}^{BMO} C_g^{BMO} - V_l k_{21}^{BMO} C_l^{BMO} + \frac{V_{max}^{Cyt_1} M_{prot} C_l^{BD}}{K_M^{Cyt_1}(1 + C_l^{BMO}/K_M^{Cyt_2}) + C_l^{BD}} - V_l C_l^{BMO} \left(\frac{V_{max}^{EH} M_{prot}}{V_l(K_M^{EH} + C_l^{BMO})} + \frac{V_{max}^{GST} M_{prot}}{V_l(K_M^{GST} + C_l^{BMO})} + \frac{V_{max}^{Cyt_2} M_{prot}}{V_l[K_M^{Cyt_2}(1 + C_l^{BD}/K_M^{Cyt_1}) + C_l^{BMO}]} + k_{hy} + k_{gsh} C^{GSH} \right) \quad (4)$$

V_l and V_g are the volumes (ml) of the liquid phase and gas phase respectively. C_l and C_g are the concentrations (μmol/ml) in the liquid or gas phase respectively of BD or BMO (indicated by superscript). M_{prot} (mg) is the total amount of protein in the reaction mixture. V_{max} and K_M are the Michaelis−Menten constants related to the different enzymic reactions. The maximal metabolic rate (V_{max}) is expressed in units of μmol/mg protein/min and K_M is expressed in mM. The superscript indicates the reaction type: Cyt_1, cytochrome P450-mediated oxidation of BD to BMO; Cyt_2, cytochrome P450-mediated oxidation of BMO to BDE; EH, hydrolysis of BMO by epoxide hydrolases; GST, conjugation of BMO with GSH by glutathione S-transferases. k_{hy} (min^{-1}) and k_{gsh} (ml/μmol/min) are the first-order non-enzymic hydrolysis and second-order conjugation rates of BMO respectively. k_{12} and k_{21} are the first-order exchange rates (min^{-1}) between the gas and liquid phases in the reaction vial. C^{GSH} (mM) is the concentration of GSH in the reaction mixture.

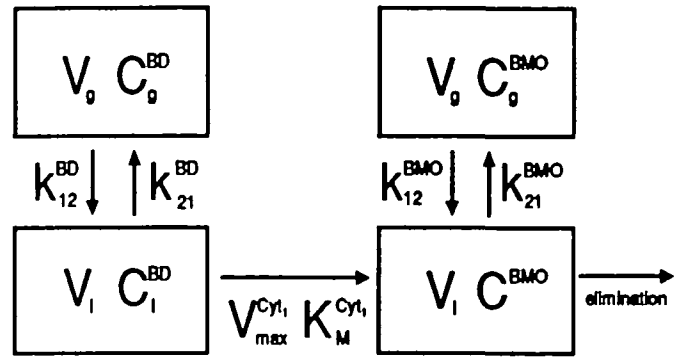

Fig. 1. Two-compartment model for describing BD and BMO distribution and metabolism in the *in vitro* systems used in estimating the microsomal oxidation (cyt) of BD. The boxes represent compartments (g = gas phase and l = liquid phase) in the sealed reaction vials. *V* corresponds to the volume of the gas or liquid phase, *C* corresponds to the concentration of BD or BMO in the gas or liquid phase, k_{12} and k_{21} are the first-order rate constants describing the transfer of BD or BMO from the gas to liquid and liquid to gas phases respectively. V_{max} and K_M are the Michaelis−Menten rate constants describing the maximum metabolic rate and BD substrate concentration of half-maximum velocity respectively. The arrow identified as elimination represents the sum of the metabolic and non-enzymic processes for BMO elimination as described in equation (4).

The differential equations (equations 1−4) were integrated using the Advanced Simulation Language software of Mitchell and Gauthier, Associates (Concord, MA) and a VAX 4000/300 computer (Digital Equipment Corp.). Simusolv Software (Dow Chemical Co., Midland, MI) was used to obtain optimal rate constants and standard deviations for the rate constants. The standard deviation gives a measure of the uncertainty in the computer estimate of the rate constants. Simulations of the various experiments were conducted. The predicted concentrations of BD and BMO in the gas phase (i.e. C_g^{BD} and C_g^{BMO}) resulting from model simulations were compared to experimentally determined values for C_g^{BD} and C_g^{BMO} measured by GC. The magnitude of the rate constants was varied until results of model simulations approximated the experimental data. The log likelihood function was used as the objective function for determining the optimum set of parameter estimates.

Because the equations described above relied on information for a number of rate constants, the following sequence was used to analyze data. First the distribution constants (k_{12} and k_{21}) for BD and BMO were determined. Results from experiments employing heat-inactivated microsomes or phosphate buffer were used to define the distribution constants k_{12} and k_{21} for BD and BMO. Model simulations of BD and BMO in the gas phase were compared to experimental values for C_g^{BD} and C_g^{BMO}. In these simulations, other rate constants in equations (1)−(4) were set to zero (i.e. V_{max}). Once optimum values for k_{12} and k_{21} were determined, they were used for subsequent simulations. The hydrolysis rate of BMO (k_{hy}) in buffer was determined by comparing model predictions to time course data for C_g^{BMO} in experiments in which BMO was injected into vials containing phosphate buffer. The distribution constants k_{12}^{BMO} and k_{21}^{BMO} defined previously were used in equation (4) and other rate constants were set to zero in order to determine k_{hy}.

With the non-enzymic rate constants set, the metabolic rate constants were determined first for BMO. The enzymic rate constants for BMO hydrolysis, V_{max}^{EH} and K_M^{EH}, were determined by comparing model predictions for BMO disappearance from the gas phase (C_g^{BMO}) to experimentally determined values obtained from *in vitro* incubations in which NADPH was omitted from the reaction mixture. The absence of NADPH in reactions prevented enzymic oxidation of BMO, thereby permitting estimation of the enzymic hydrolysis rate constants independently. With the rate constants for hydrolysis known, rate constants for cytochrome P450-mediated oxidation of BMO to BDE (i.e. $V_{max}^{Cyt_2}$, $K_M^{Cyt_2}$) were determined. The rate constants were adjusted until model simulations for C_g^{BMO} agreed with experimentally determined concentrations of BMO in the gas phase obtained in incubations in which NADPH was added to reactions.

With values for the rate constants describing BMO oxidation and hydrolysis incorporated into equation (4), the rate constants for the metabolism of BD

could then be estimated. Experimentally determined values for BD and BMO concentrations in the gas phase (i.e. C_g^{BD} and C_g^{BMO}) obtained in incubations with microsomal protein, NADPH and varying initial concentrations of BD were compared to results from model simulations in which only V_{max}^{Cyt} and K_M^{Cyt}, the rate parameters for BD oxidation, were varied. The rate constants were adjusted until optimal simulations for BD disappearance from the gas phase and BMO appearance in the gas phase were achieved, as compared to the experimentally determined data (i.e. C_g^{BD} and C_g^{BMO}).

Enzymic and non-enzymic rate constants for reaction of GSH with BMO were obtained by comparing simulations to a separate set of experiments in which the formation of BMO−GSH conjugates was quantitated by measuring the concentration of GSH conjugates in the reaction liquid as a function of the initial BMO concentration in the reaction mix. Non-enzymic second-order rate constants were derived by comparing model simulations for GSH conjugate formation with results obtained when GSH was incubated with BMO in buffer.

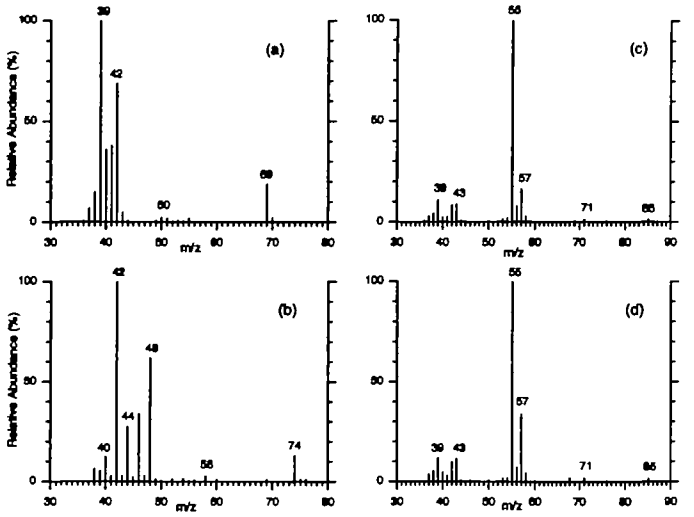

Fig. 2. Mass spectra of (a) authentic butadiene monoepoxide standard; (b) head-space sample of a reaction of B6C3F1 mouse liver microsomes with butadiene-d_6; (c) authentic butadiene diepoxide standard; (d) organic extract of a reaction of B6C3F1 mouse liver microsomes with butadiene monoepoxide. The incubation conditions and analytical procedures are described in the text.

Results

Mass spectral analysis of BD epoxides

Analyses of head-space samples after a 30 min incubation of BD-d_6 (10 000 p.p.m. initial concentration injected into head-space) with liver microsomes of B6C3F1 mice were performed by GC−MS. Figure 2(a) shows the mass spectrum of the authentic BMO standard and of the head-space sample (Figure 2b). The mass spectrum of the authentic BMO metabolite standard (Figure 2a) had a parent ion at *m/z* 69 $[(M-1)^+]$ and exhibited a prominent loss of 28 mass units $[(M-CO)^+]$ and 31 mass units $[(M-H_2COH)^+]$. The mass spectrum of the head-space sample was consistent with that expected for BMO containing six deuteriums and exhibited a prominent loss of 28 mass units $[(M-CD)^+]$ and 34 mass units $[(M-D_2COD)^+]$. These data indicate that BMO is a volatile metabolite formed in reaction mixtures containing BD. Reaction mixtures containing B6C3F1 liver microsomes, NADPH and 1 mmol BMO were analyzed for the presence of BDE by GS−MS following extraction of the reaction mixture with methylene chloride. The mass spectrum is shown in Figure 2(d) and has a fragmentation pattern identical to that of the authentic BDE metabolite standard (Figure 2c).

Microsomal metabolism of BD

The cytochrome P450 contents of human, rat and mouse liver microsomes were 0.16 ± 0.097, 0.65 ± 0.04 and 0.51 ± 0.17 nmol P450/mg microsomal protein (mean ± SD) respectively. We were unable to quantitate accurately the cytochrome P450 content of lung microsomes from any of the three animal species.

Heat-inactivated liver microsomes were used to estimate the distribution parameters k_{12}^{BD} and k_{21}^{BD} described in equations (1) and (2). The calculated distribution coefficient $(k_{12} \cdot V_g/k_{21} \cdot V_l)$ was 0.105 ± 0.015, indicating a 10-fold higher BD concentra-

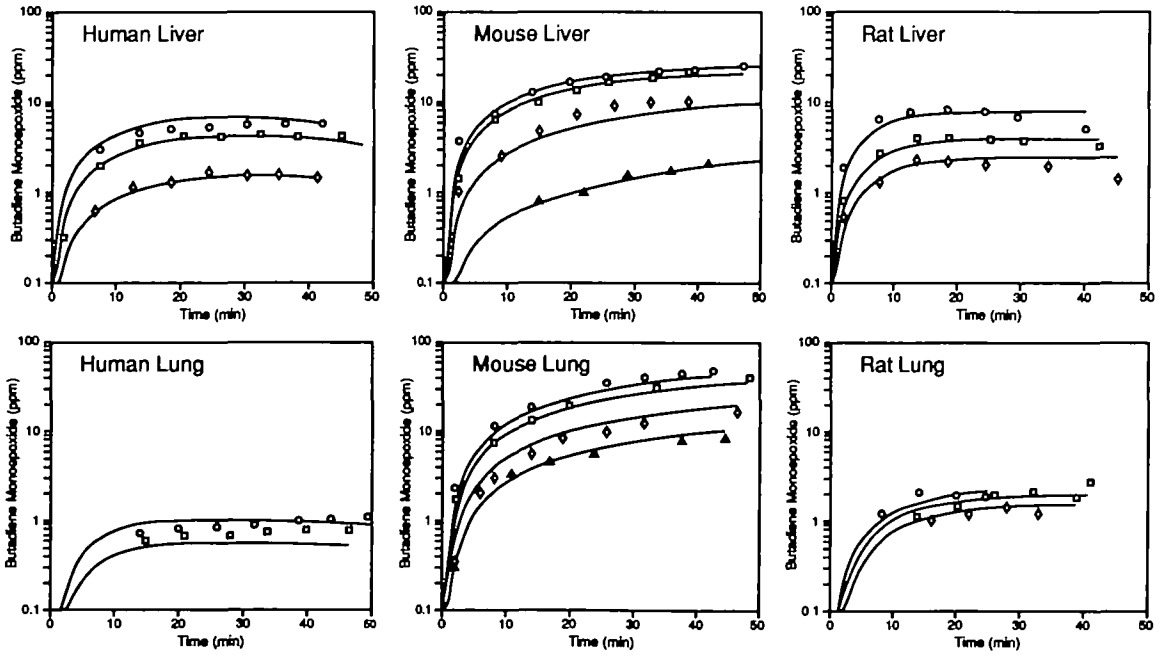

Fig. 3. Model simulations (lines) of butadiene monoepoxide appearance in the head-space following incubations of multiple butadiene concentrations with liver microsomes of humans (1.4 mg microsomal protein/ml), mice (2.0 mg microsomal protein/ml) and rats (2.0 mg microsomal protein/ml), and lung microsomes of humans (1.2 mg microsomal protein/ml), mice (1.4 mg microsomal protein/ml) and rats (1.8 mg microsomal protein/ml). The incubation conditions and analytical procedures are described in the text. The lines and their associated data sets represent separate experiments at different starting butadiene concentrations. Each graph shows representative data (symbols) and model simulations (lines) for butadiene monoepoxide appearance in the head-space.

tion in the head-space (i.e. gas phase) than in the microsomal phase. The values for k_{21}^{BD} and k_{12}^{BD} were used directly in the equations described in Materials and methods and for the analysis of kinetic parameters for the reactions.

The initial rate of BD oxidation in liver and lung microsomes was linear with protein content over the range of 1.0–9.0 mg protein/ml and with time for up to 30 min (data not shown). For the enzyme-mediated reactions using liver and lung microsomes, both the disappearance of BD from the gas phase (data not shown) and the appearance of BMO in the gas phase were measured (Figure 3). The previously determined parameters of BMO metabolism (see below) were incorporated into equations used to describe the *in vitro* system (equations 1–4). The equations were then used to estimate the Michaelis–Menten constants for BD oxidation as described previously. A representative data set of the BMO formation–time curves for liver and lung microsomes from all three species are shown in Figure 3 and the Michaelis–Menten parameters are listed in Table I. The lines shown on the graphs represent model simulations using equations (1)–(4). The model adequately described both BD disappearance from the head-space (data not shown) and the BMO appearance in the head-space of reaction vials containing either liver or lung microsomes from all three species.

Table I. Kinetic constants for the oxidation of 1,3-butadiene or butadiene monoepoxide[a]

	$V_{max}^{Cyt_1}$ (nmol/mg protein/min)	$K_M^{Cyt_1}$ (μM)	$V_{max}^{Cyt_1}/K_M^{Cyt_1}$[c]
Liver microsomes			
Human	1.18 ± 0.61	5.14 ± 2.59	230
Mice (BD → BMO)	2.59 ± 0.06	2.00 ± 0.17	1295
(BMO → BDE)[b]	0.20 ± 0.06	15.6 ± 3.45	12.8
Rat	0.59 ± 0.12	3.75 ± 0.20	157
Lung microsomes			
Human	0.15 ± 0.04	2.00 ± 0.15	75
Mice	2.31 ± 0.26	5.01 ± 0.67	461
Rat	0.16 ± 0.01	7.75 ± 1.86	20.6

[a]Values are mean ± SD derived from model simulations.
[b]Only mouse liver microsomes metabolized butadiene monoepoxide (BMO) to butadiene diepoxide (BDE) at rates that resulted in measurable BDE levels. The values represent $V_{max}^{Cyt_2}$, $K_M^{Cyt_2}$ and $V_{max}^{Cyt_2}/K_M^{Cyt_2}$.
[c]Values are in units of $l \cdot$nmol/(min·mg protein·mmol).

The $V_{max}^{Cyt_1}$ for BD oxidation to BMO for human liver microsomes was about one-half that observed with mouse liver microsomes and 2-fold higher than in rat liver microsomes (Table I). The apparent $K_M^{Cyt_1}$s for BD oxidation in liver microsomes from all three species were similar and ranged from 2 to 5 μM. The oxidation of BMO to BDE was negligible in reactions using liver or lung microsomes from Sprague–Dawley rats or humans and could not be quantitated. Only mouse liver microsomes oxidized BMO to BDE at rates that could be quantitated (Table I). The $V_{max}^{Cyt_2}$ for this reaction was at least 10-fold lower than the $V_{max}^{Cyt_1}$ for the oxidation of BD in mouse liver microsomes. The apparent $K_M^{Cyt_2}$ for the oxidation of BMO to BDE in mouse liver microsomes was nearly 8-fold higher than the apparent $K_M^{Cyt_1}$ for BD oxidation to BMO. There were some striking differences in the calculated $V_{max}^{Cyt_1}/K_M^{Cyt_1}$ (29) among the three species. The calculated $V_{max}^{Cyt_1}/K_M^{Cyt_1}$ for BD oxidation in mouse liver microsomes was 6-fold greater than for rat and human liver microsomes. The calculated $V_{max}^{Cyt_2}/K_M^{Cyt_2}$ for BMO oxidation was ~1% of the $V_{max}^{Cyt_1}/K_M^{Cyt_1}$ for BD oxidation in mouse liver microsomes.

With the exception of the mice, lung microsomes displayed considerably lower capacity to metabolize BD than did liver microsomes (Figure 3, Table I). For example, $V_{max}^{Cyt_1}$ for BD oxidation in lung microsomes of humans and rats were similar and about 10 and 4 times lower respectively than measured in

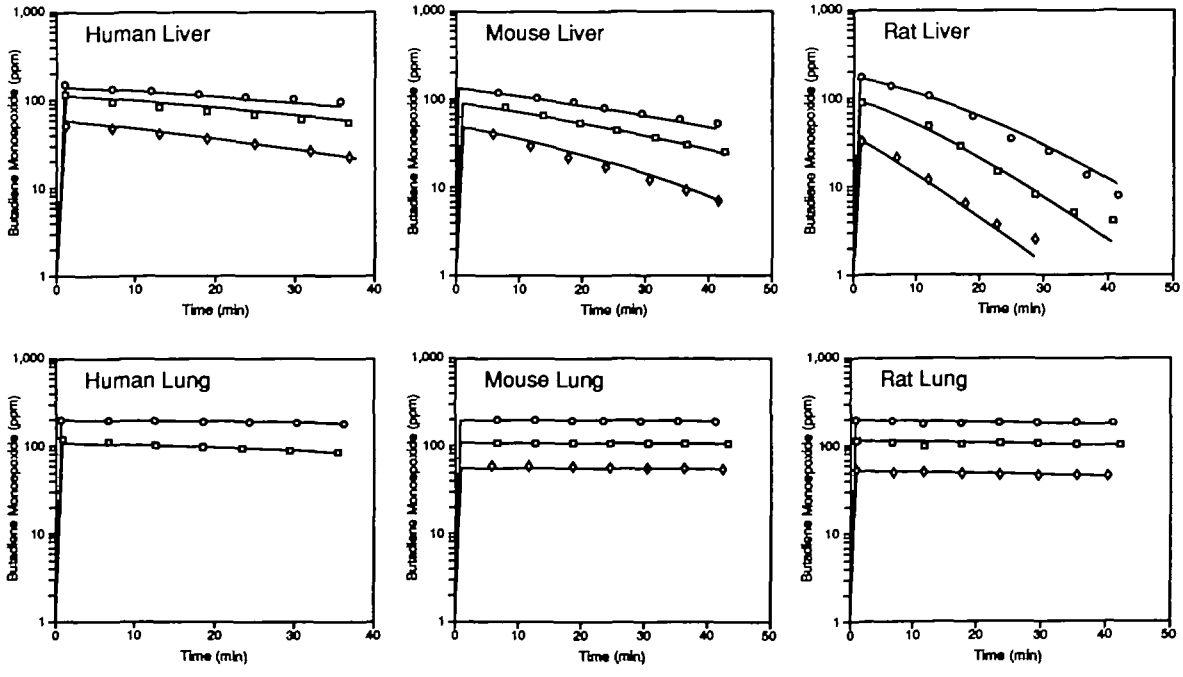

Fig. 4. Model simulations (lines) of enzyme-mediated hydrolysis of butadiene monoepoxide in liver (**upper panel**) and lung (**lower panel**) microsomes of humans, mice and rats. The incubation conditions and analytical procedures are described in the text. The lines and their associated data sets represent separate experiments at different starting butadiene monoepoxide concentrations. Each graph shows representative data (symbols) and model simulations (lines) for butadiene monoepoxide hydrolysis. Protein concentrations were liver: human, 1.4 mg microsomal protein/ml; mice and rats, 2.0 mg microsomal protein/ml; lung: human, 1.2 mg microsomal protein/ml; mice, 1.4 mg microsomal protein/ml; rats, 1.8 mg microsomal protein/ml.

Table II. Kinetic constants and first-order elimination rates for the hydrolysis of butadiene monoepoxide[a]

Liver microsomes	V_{max}^{EH} (nmol/mg protein/min)	K_M^{EH} (mM)	V_{max}^{EH}/K_M^{EH}[c]	K_i(TCPO) (μM)
Human[b] (high)	58.1 ± 4.0	1.65 ± 0.12	35	0.10 ± 0.01
(median)	18.5 ± 4.1	0.58 ± 0.15	32	0.10 ± 0.01
(low)	9.2 ± 2.2	0.24 ± 0.10	38	0.26 ± 0.02
Mice	5.79 ± 0.25	1.59 ± 0.03	3.6	1.45 ± 0.10
Rat	2.48 ± 0.05	0.26 ± 0.01	9.5	0.10 ± 0.03
Lung microsomes	k_{hy}[d] (min^{-1} mg $protein^{-1}$) × 10^3		K_i(TCPO)	
Human[e]	4.00 ± 0.54		+[f]	
	3.19 ± 0.33		NM[g]	
	7.55 ± 0.43		NM	
Rat	1.32 ± 0.61		+	
Mice	1.86 ± 0.014		+	

[a]Values are mean ± SD derived from model simulations.
[b]Three of the 12 human liver samples were used for the kinetic analyses. Selection of the samples was as described in Materials and methods.
[c]Values are in units of nmol·l/(min·mg protein·mmol).
[d]k_{hy} = normalized first-order rate constant for enzymic hydrolysis of butadiene monoepoxide.
[e]Data shown are for each of the three lung samples analyzed.
[f]+ = inhibition with TCPO was detected, but K_i could not be calculated.
[g]NM = not measured.

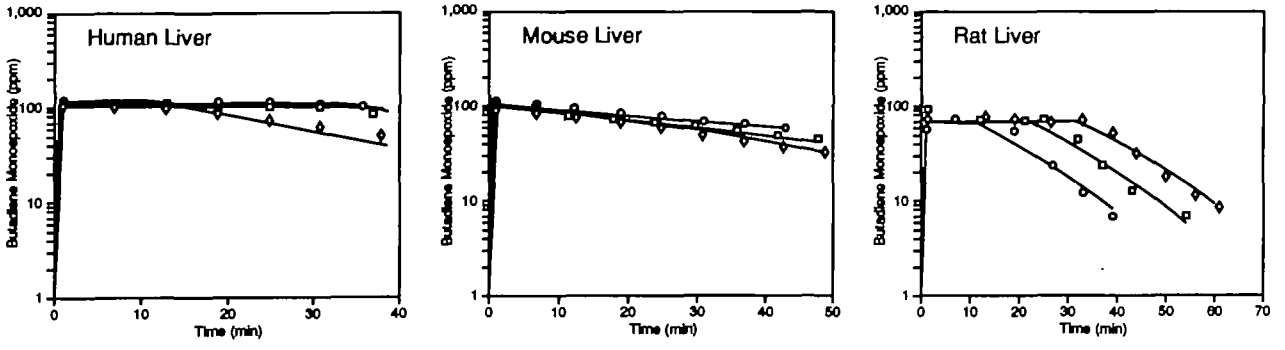

Fig. 5. Inhibition of enzyme-mediated hydrolysis of butadiene monoepoxide (100 p.p.m.) by 1,1,1-trichloropropene oxide (TCPO). ◇, 0.25 μM TCPO; □, 1.1 μM TCPO; ○, 3.6 μM TCPO. Protein concentrations of human, mouse and rat liver microsomes in reaction flasks were 1.4, 2.0 and 2.0 mg microsomal protein/ml respectively.

liver microsomes of the same species. The $V_{max}^{Cyt_i}$ for mouse lung microsomal metabolism of BD was similar to that measured in mouse liver microsomes. Apparent $K_M^{Cyt_i}$s for BD oxidation in lung tissue of all three species ranged from 2 to 8 μM. The calculated $V_{max}^{Cyt_i}/K_M^{Cyt_i}$ for lung microsomal oxidation of BD was less than liver microsomal metabolism of BD for all three species.

Microsomal metabolism of BMO

The distribution parameters k_{12}^{BMO} and k_{21}^{BMO} (see equations 3 and 4) were determined using heat-inactivated liver and lung microsomes. The calculated distribution coefficient for BMO ($k_{12} \cdot V_g/k_{21} \cdot V_l$) was 67.2 ± 0.5 (mean ± SD), indicating that BMO partitioned extensively into the reaction mixture. The k_{12}^{BMO} and k_{21}^{BMO} values were used directly in the equations described in Materials and methods for the analysis of kinetic parameters for the reactions. The spontaneous hydrolysis rate (k_{hy}) of BMO in 0.1 M phosphate buffer (pH 7.4) was (7.75 ± 2.03) × 10^{-4} min^{-1} (mean ± SD). This rate of ~0.08%/min indicates that spontaneous hydrolysis does not contribute significantly to the decline of BMO in the head-space in experiments designed to assess enzyme-mediated metabolism of BMO.

Initial rates of enzymic hydrolysis of BMO in liver and lung microsomes were linear with protein content over the range 0.2–10 mg/ml and with time for up to 30 min (data not shown). Enzyme-mediated hydrolysis of BMO was not detected in cytosolic fractions of liver and lung from any of the three species. All 12 of the human liver samples were assessed for their ability to metabolize BMO using one initial BMO concentration (100 p.p.m.). The normalized first-order rate constants for the 12 liver samples, which varied between 0.020 and 0.068 min^{-1} mg $protein^{-1}$, were then rank-ordered and three samples (high, median, low activity) were selected for detailed studies of BMO kinetics (see below). Representative data sets of the BMO hydrolysis–time curves for liver and lung microsomes of humans, rats and mice are shown in Figure 4. In all cases, results of model simulations adequately described the decline in BMO concentration in the head-space due to enzymic hydrolysis.

Table II shows the Michaelis–Menten constants (K_M^{EH}, V_{max}^{EH}) for BMO hydrolysis by human, rat and mouse liver and lung microsomes. In the three human liver samples used for the detailed kinetic experiments, V_{max}^{EH} ranged from 9 to 60 nmol/mg protein/min and apparent K_M^{EH}s ranged from 0.2 to 1.6 mM. In contrast, V_{max}^{EH} determined from reactions using rodent liver microsomes was one-half or less than that measured in human liver samples. Apparent K_M^{EH}s for mice were ~7- to 8-fold

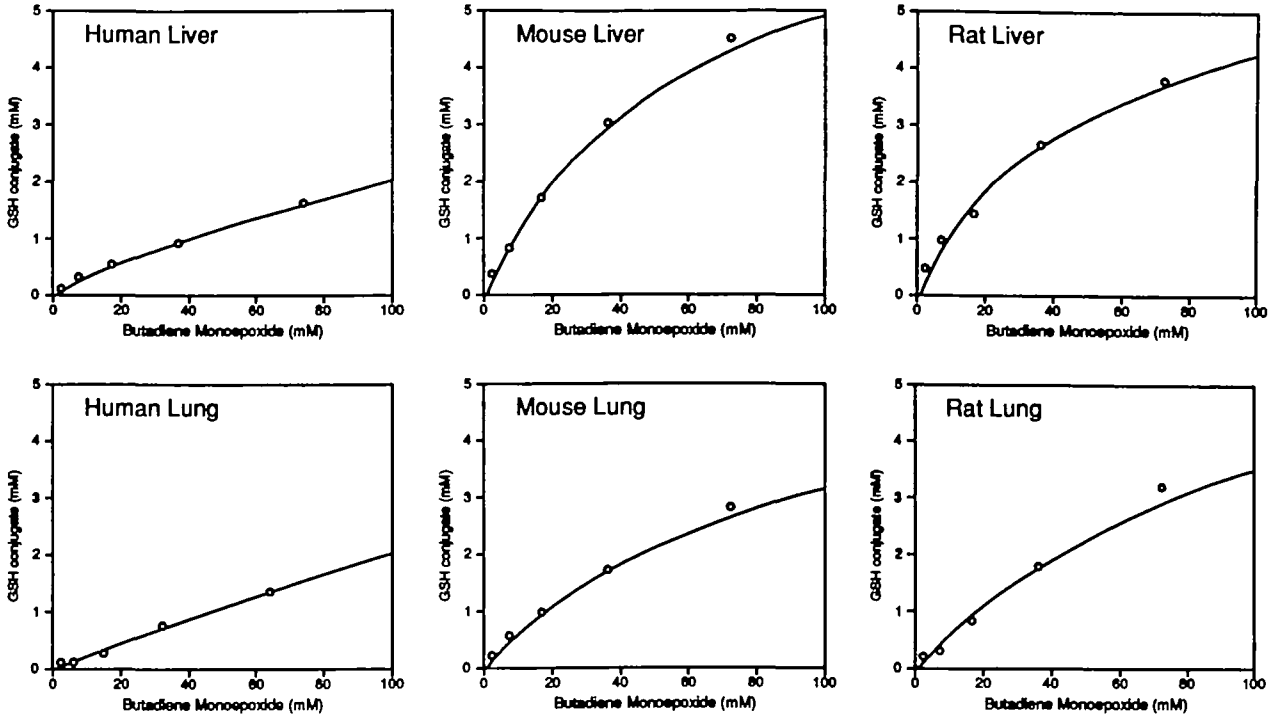

Fig. 6. Formation of butadiene monoepoxide–GSH conjugates in reactions containing liver and lung cytosol from humans, mice and rats. Protein concentrations in all reactions were 1 mg cytosolic protein/ml. Incubation times were 10 min. Data points represent data for both the formation of *S*-(1-hydroxy-3-buten-2-yl)glutathione and *S*-(2-hydroxy-3-buten-1-yl)glutathione combined. The lines are model simulations for the reaction.

higher than the K_M^{EH}s observed in rats. A comparison of the calculated V_{max}/K_M reveals some striking differences across species (Table II). For example, for the three human liver samples, calculated V_{max}/K_Ms ranged from 32 to 38, whereas in rodents calculated V_{max}/K_Ms ranged from 4 to 10.

Lung microsomal preparations from all three species showed considerably less capacity to hydrolyze BMO enzymically (Figure 4). This was evidenced by the more rapid decline in BMO concentration in the head-space of the reaction vials when liver microsomes were incubated with BMO in the absence of NADPH compared to lung microsomes. Over the concentration range investigated, BMO hydrolysis in lung microsomes was best described as a first-order process (Table II).

Significant differences among the species were seen in the inhibition of enzymic hydrolysis of BMO by TCPO (Figure 5, Table II). The inhibition constant, K_i (assuming a competitive mechanism), in liver microsomes of B6C3F1 mice was 1.45 μM, ~10 times higher than the K_i in rat or human liver microsomes (Table II).

Conjugation of BMO with GSH

Enzyme-mediated conjugation of GSH with BMO in human and rodent liver cytosol and rodent lung cytosol could best be described by Michaelis–Menten kinetics (Figure 6, Table III). The data presented in Figure 6 reveal that the model adequately simulated BMO–GSH conjugate formation in liver and lung cytosolic fractions from all three species. The actual data plotted represent the sum of the two adducts formed upon conjugation of BMO with GSH, *S*-(2-hydroxy-3-buten-1-yl)glutathione and *S*-(1-hydroxy-3-buten-2-yl)glutathione. These conjugates were formed in a ratio of 1:1–2. The V_{max}^{GST} in mouse liver cytosolic fractions was ~2-fold higher than in rat liver cytosol (Table III). Only one of the two human liver samples analyzed displayed Michaelis–Menten kinetics and had a V_{max}^{GST} of 1/5–1/10 of that observed in rodents. Mouse liver cytosolic apparent K_M^{GST}s were ~3-fold higher than rats and humans. V_{max}^{GST}s in rodent tissue were 20 and 50% of the values measured in livers for rats and mice respectively. None of the human lung cytosol samples displayed Michaelis–Menten reaction kinetics. The calculated V_{max}^{GST}/K_M^{GST} in rodent liver cytosol was ~4-fold higher than the calculated V_{max}^{GST}/K_M^{GST} for the single human sample.

Table III. Kinetic constants for conjugation of butadiene monoepoxide with glutathione[a]

Sample	V_{max}^{GST} (nmol/mg protein/min)	K_M^{GST} (mM)	V_{max}^{GST}/K_M^{GST}[c]
Liver cytosol			
Human[b]	45.1 ± 5.8	10.4 ± 1.04	4.3
Mice	500 ± 64	35.3 ± 6.2	14
Rat	241 ± 3	13.8 ± 0.3	17
Lung cytosol			
Human[d]	–	–	–
Mice	273 ± 31	36.5 ± 5.5	7.5
Rat	44.2 ± 12.6	17.4 ± 6.2	2.5

[a]Values are the mean ± SD derived from model simulations.
[b]Two of the 12 human liver samples were used for kinetic analyses. Selection of the samples were as described in Materials and methods. One of the samples displayed Michaelis–Menten kinetics and in the other sample, the reaction was best described by a k_{gsh} = (2.56 ± 0.22) × 10^{-4} l/mmol/min/mg protein (mean ± SD).
[c]Values are in units of $l \cdot$nmol/(min·mg protein·mmol).
[d]None of the human lung cytosolic fractions displayed Michaelis–Menten reaction kinetics. The reactions were best described by a k_{gsh} = (2.56 ± 0.22) × 10^{-4} l/mmol/min/mg protein (mean ± SD).

Microsomal GSH transferase activity with BMO as substrate for both human and mouse lung and liver was similar to the spontaneous conjugation rate of BMO with GSH [k_{gsh} = (2.01 ± 0.06) × 10^{-4} l/mmol/min; mean ± SD]. Rat liver and lung microsomal-catalyzed conjugation of BMO with GSH

Table IV. Rate constants for the conjugation of butadiene monoepoxide with glutathione[a]

	k_{gsh} (l/mmol/min/mg protein) × 10^4
Liver microsomes	
Human[b]	3.71 ± 0.30
	2.21 ± 0.26
Mice	2.94 ± 0.30
Rat	7.92 ± 0.21
Lung microsomes	
Human	1.98 ± 0.26
Mice	2.09 ± 0.25
Rat	5.55 ± 0.29

[a]Values are mean ± SD derived from model simulations.
[b]Two of the 12 human liver samples were used for determination of k_{gsh}. Selection of the samples was as described in Materials and methods.

Table V. 6-Hydroxylation of chlorzoxazone in liver and lung microsomes

	6-Hydroxylation of chlorzoxazone (nmol/min/mg protein)[a]
Liver microsomes	
Human	0.59 ± 0.29 (n = 12)[b]
Mice	0.43 ± 0.11 (n = 9)
Rat	0.36 ± 0.12 (n = 8)
Lung microsomes	
Human	0.05 ± 0.03 (n = 3)
Mice	0.18 ± 0.10 (n = 2)
Rat	0.12 ± 0.10 (n = 3)

[a]Values are mean ± SD.
[b]Numbers in parentheses represent the number of samples used for the analysis.

was only 2–3 times greater than the spontaneous conjugation rate. The normalized second-order rate constants from all three species ranged from 2 to 8 × 10^{-4} l/min/mg protein (Table IV).

Hydroxylation of chlorzoxazone in human liver microsomes

Table V shows the rates of chlorzoxazone 6-hydroxylation in liver and lung microsomes of mice, rats and humans. Liver microsomes from all three species metabolized chlorzoxazone to a similar extent, with values ranging from about 0.4 to 0.6 nmol/mg protein/min. Lung microsomes from all three species metabolized chlorzoxazone at significantly lower rates than liver microsomes and the coefficient of variation was considerably larger in these tissues than in the liver samples. Since chlorzoxazone has been reported to be a highly specific substrate for human liver cytochrome P450 2E1 (25,26), we compared the ability of the 12 human liver microsomes to metabolize BD and chlorzoxazone (Figure 7). There was a good correlation (r = 0.88) between these two substrates for the 12 human liver samples analyzed.

Discussion

An understanding of the mechanisms by which BD induces tumors in rats and mice is essential for extrapolating to humans, a species for which BD carcinogenic potency is at present unknown. It is likely that one of the critical biochemical determinants of BD-induced carcinogenicity is the extent to which BD is activated to epoxide metabolites that can react with DNA.

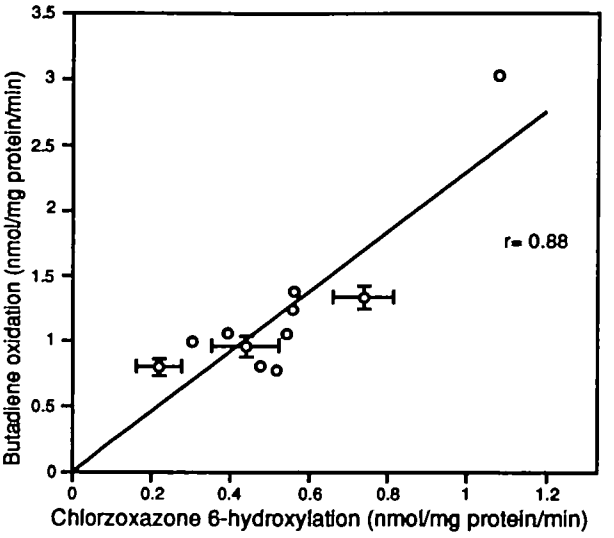

Fig. 7. Correlation of the oxidation of BD to BMO and oxidation of chlorzoxazone to 6-hydroxychlorzoxazone in human liver microsomal samples. Each point represents an individual sample. Data points with error bars represent the mean ± SD.

A number of studies suggest that species differences exist in the *in vivo* metabolism of BD and several investigators have suggested that these differences explain, in part, the observed species differences in BD carcinogenicity (15,16,18,30). While the available data on BD metabolism in rodents offers insights into differences in carcinogenic susceptibility, they are of limited use in extrapolating to the human situation. The present paper has provided a comprehensive, quantitative, interspecies comparison of the *in vitro* metabolism of BD and BMO in livers and lungs of rodents and humans.

The multiple enzymic pathways involved in BD metabolism present a challenge for quantitating rates of activation and inactivation of BD and BMO. The methodology employed in our studies enabled us to evaluate oxidation of BD to BMO and the further oxidation, hydrolysis and conjugation of BMO. Selective addition or deletion of cofactors (e.g. NADPH, GSH) enabled us to focus on specific metabolic pathways of BMO metabolism, while the head-space GC analysis method allowed us to take advantage of the volatility of BD and BMO. Kinetic constants associated with the different enzymic reactions were determined using a model that simultaneously accounts for chemical distribution between the gas head-space and liquid reaction-phase as well as changes in substrate concentration due to competing enzymic reactions.

Several studies have reported on the capacity of rodent liver microsomes to metabolize BD and BMO (20,31–35). With a few exceptions, these studies typically reported *in vitro* BD metabolism in livers from strains of rats and mice for which there are no data on BD carcinogenicity. For example, Malvoisin *et al.* (34) reported that liver microsomes from male Wistar rats metabolized BD to BMO at rates of ~63 nmol/mg protein/min, values that are 100-fold greater than the V_{max} values reported in this paper using Sprague–Dawley rat liver microsomes. Significant strain differences may exist in the *in vitro* metabolism of BD or, alternatively, the methods used to assess *in vitro* metabolism may have resulted in an overestimate of the true V_{max}. Schmidt and Löeser (20) reported that 10 000 *g* supernatant fractions from male NMRI mouse liver and lungs metabolized BD at rates of 2.7 and 5.6 nmol/g tissue/min respectively. It is difficult to compare these values directly to

Table VI. Rate constants for *in vivo* hepatic clearance of butadiene and butadiene monoepoxide[a]

	Cytochrome P450 monooxygenase[b]	Epoxide hydrolase[b]	Cytosolic glutathione S-transferase[b]	Microsomal conjugation of BMO with GSH[c]	First-order hydrolysis
Mouse	55.9 0.55[d]	0.16	0.60	0.011	0.0028
Rat	7.92	0.48	0.86	0.024	0.0022
Human	6.19	0.86	0.12	0.069	0.0014

[a]Values are in units of l/h/kg.
[b]*In vivo* V_{max} were calculated from *in vitro* V_{max} (see Tables I–III) and adjusted for interspecies differences in microsomal and cytosolic protein concentrations and liver volume. Mouse, rat and human liver microsomal concentrations were 11.6, 16.8 and 14.5 mg/g liver respectively. Mouse, rat and human liver cytosolic concentrations were 82.8, 108 and 58 mg/g liver respectively. Liver organ volumes for mice, rats and humans were 6.2, 5.0 and 3.1% of body weight respectively. *In vivo* hepatic clearance values (V/K expressed in l/h/kg) were estimated by dividing the *in vivo* V_{max} values by the apparent *in vitro* K_Ms for the reaction.
[c]For non-enzymic hydrolysis and reaction with glutathione, *in vivo* clearance was calculated using the organ fractions in footnote b. To estimate the *in vivo* clearance for reaction with glutathione a concentration of 10 mM GSH was used.
[d]Rate constant for metabolism of BMO to BDE.

those reported in this paper, but assuming 10–15 mg microsomal protein/g tissue, these values would be significantly less than the V_{max} values reported in this paper for B6C3F1 mouse liver and lung microsomes. Although no data are shown, these authors state that data developed in B6C3F1 mice are similar to that reported for NMRI mice. Based on our results for B6C3F1 mice, it is likely that the values reported by Schmidt and Löeser (20) do not represent V_{max} for the reaction.

The data presented in this paper reveal that there are significant species differences in the V_{max} observed for BD oxidation to BMO. For example, mouse liver and lung microsomes displayed a capacity for BD oxidation which exceeded that seen in either human or rat liver and lung microsomes. This was evidenced by a comparison of both the maximum velocity for the reaction, V_{max}, and V_{max}/K_M. The data reported by Elfarra *et al.* (33) for B6C3F1 mouse liver microsomal metabolism of BD to BMO are similar to the V_{max} reported for the reaction in this paper. With the exception of the mice, lung microsomal oxidation of BD occurred at rates significantly lower than for liver microsomes. The relatively high rates of BD oxidation in mouse lung microsomes may offer some insights into an explanation for the observation that lung is a target tissue in B6C3F1 mice exposed chronically to BD at concentrations as low as 6 p.p.m. (12). BD does not induce lung tumors in rats (13), even at much higher BD exposure concentrations.

Only mouse liver microsomes were capable of metabolizing BMO to BDE at rates that could be quantitated in our system. BDE is mutagenic (36) and carcinogenic (37) and there have been conflicting reports as to whether animal tissues can metabolize BMO to BDE. For example, Malvoisin and Roberfroid (35) reported the production of BDE in rat liver microsomes, but Wistuba (38) could not confirm these findings. The results reported in this paper provide definitive data, based on MS analysis, on the formation of BMO in mouse liver microsomes. BDE is also formed in rat and human tissues but the methodology employed in these studies lacked sufficient sensitivity to quantify the rate constants. Bond *et al.* (16) reported blood levels of a metabolite tentatively identified as either BDE or 3,4-dihydroxy-but-1-ene (18) in Sprague–Dawley rats that were at least 3–5 times lower than blood levels in B6C3F1 mice exposed to 70 p.p.m. BD for 6 h. Thus, *in vivo* evidence is consistent with formation of BDE in rats and mice. The V_{max} for metabolism of BMO to BDE in mouse liver microsomes was nearly 10-fold lower than the V_{max} for BD oxidation and the K_M for BMO oxidation to BDE was over 7-fold greater than the K_M for BD oxidation. These data suggest that BMO is a poorer substrate than BD.

Guengerich and Shimada (39) have summarized a number of *in vitro* approaches that can be used to elucidate the roles of individual P450s in the oxidation of chemicals and toxicants, including correlation analysis, selective inhibition and stimulation, immunoinhibition, enzyme purification and cDNA-based expression. We employed correlation analysis to assess whether cytochrome P450 2E1 is involved to a significant extent in the initial oxidation of BD to BMO in human liver microsomes. Beaune *et al.* (40) suggested that if the same enzyme is carrying out both reactions under consideration, then the rates should be correlated when compared in a series of microsomal preparations containing varying levels of the enzyme. Peter *et al.* (26) have previously reported excellent correlations between rates of chlorzoxazone 6-hydroxylation and immunochemically quantified cytochrome P450 2E1. In our studies, when the catalytic activities for BD oxidation and chlorzoxazone 6-hydroxylation were measured in 12 different human liver microsomal preparations, good correlation for the two enzyme activities was seen. P450 2E1 appears to be a major, if not the principal, P450 enzyme responsible for oxidation of BD to BMO. However, experiments employing specific inhibitors (or antibodies) of P450 2E1 will be necessary to assess definitively the role of this isoenzyme in BD oxidation. The observation that P450 2E1 is a major isozyme for BD oxidation is consistent with the hypothesis of Guengerich *et al.* (25) that low mol. wt compounds such as vinyl chloride, acrylonitrile and dichloropropane are preferential substrates for P340 2E1.

Two putative detoxication enzymic reactions can occur with BMO, hydrolysis by epoxide hydrolase and conjugation with GSH by glutathione transferase. The results from our studies reveal that liver and lung tissues from all species can detoxify BMO by both pathways. In general, human liver microsomes hydrolyzed BMO at greater rates than either rats or mice, as evidenced by the higher V_{max} and V_{max}/K_M. While there was a considerable range of epoxide hydrolase activities in liver microsomes of the three human samples investigated V_{max} = 9–58 nmol/mg protein/min, values for the human samples were at least 2-fold greater than the V_{max} for rats and mice. The value reported by Kreuzer *et al.* (21) for epoxide hydrolase-catalyzed hydrolysis of BMO by microsomes from a single human liver sample (V_{max} = 14 nmol/mg protein/min) falls within the range of values for V_{max} in human liver microsomes reported in this paper. Our results on GSH transferase-mediated conjugation of

BMO with GSH are consistent with the data reported for purified human placental GSH transferase-catalyzed conjugation of BMO (41). Sharer *et al.* (41) reported that purified human placental GSH transferase (π) metabolized BMO to two reaction products, *S*-(1-hydroxy-3-buten-2-yl)glutathione and *S*-(2-hydroxy-3-buten-1-yl)glutathione, with an apparent V_{max} and K_M of 500 nmol/mg protein/min and 10 mM respectively. In our studies, only liver cytosolic fraction from all three species displayed GSH transferase activity when BMO was the substrate, an observation similar to that reported by Kreuzer *et al.* (21) for Sprague–Dawley rat liver cytosol. Values for V_{max}/K_M reported by Kreuzer *et al.* (21) for rodents and the single human liver sample were similar to the values reported in this paper. For all three species, apparent K_Ms for hydrolysis and GSH conjugation were significantly greater than for BD oxidation and, in the case of mice, BMO oxidation.

Significant species differences exist not only in the rates of BD oxidation but also in both the rates and relative affinities of the pathways for BMO metabolism. In general, the maximum capacity for BD oxidation is highest for mice compared to rats and humans. Detoxication capacity for BMO varies depending on the enzyme under consideration. For example, enzymic hydrolysis is highest for humans compared to mice or rats, whereas capacity for GSH conjugation is highest for mice compared to humans or rats. Enzyme affinities also vary when compared across species or as competing reactions for a single substrate. For example, in mouse liver microsomes the oxidation pathway has a much higher affinity for BMO compared to either of the detoxication pathways.

The next step in comparing BD metabolism across species is to develop a methodology to scale rate constants developed *in vitro* to predict *in vivo* behavior. Rates for *in vivo* hepatic clearance (*V/K*, Table VI) were calculated from *in vitro* data by adjusting for differences in microsomal protein content and organ weights across species. Because of the low solubility of BD and the relatively high K_M for oxidation, metabolism of BD and BMO will most likely be governed by the ratio V_{max}/K_M rather than V_{max}. *In vivo* clearance values can be used to estimate steady-state blood concentrations of BD and BMO following exposure to low concentrations of BD. For example, with a BD blood/air partition coefficient of 1.5 and tissue/blood partition coefficients of ~1.0 (unpublished observations), steady-state concentrations of BD in blood and liver should be on the order of 3 μM after exposure to 70 p.p.m. (see Appendix). Due to the low enzymic affinities (large values for K_M), rates of BMO metabolism will be a function of V_{max}/K_M. Using the hepatic clearance values for BMO in Table VI and steady-state BD blood concentrations described above, steady-state BMO blood concentrations for rats and mice were estimated to be ~5.1 and 10 μmol BMO/l respectively (see Appendix). These values are higher than the measured values of BMO in blood of male B6C3F1 mice and male Sprague–Dawley rats exposed to 70 p.p.m. BD for 6 h (16). BMO blood concentrations in mice ranged from 0.9 to 2 μmol/l, whereas average values for rats were ~0.4 μmol/l (16). There are two possible reasons why the predicted steady-state BMO blood concentrations are higher than the values reported by Bond *et al.* (16). The first relates to the fact that these calculations are for steady-state levels of BMO and given the relatively high BMO blood/air partition coefficient (P_b = 60; unpublished observations), it is unlikely that steady-state concentrations of BMO were achieved in the Bond *et al.* (16) studies. The second reason relates to the fact that our calculations assumed that non-enzymic BMO hydrolysis and GSH conjugation occurred only in the liver and it is likely that these reactions occur in extrahepatic tissues as well. Both of these factors would reduce the predicted BMO blood concentrations.

The *in vivo* clearance constants in Table VI also suggest that the overall activation/detoxication ratio for BD will be very different in rats, mice and humans. This ratio can be calculated by dividing the *V/K* for BD oxidation in livers of all three species by the sum of the clearance values for BMO and Table VI. These ratios are 72, 5.8 and 5.9 for mice, rats and humans respectively, and suggest that at concentrations below the K_M for the reactions, mice have a significantly higher ratio of activation/detoxication than do either rats or humans. The difference between mice and humans is at least an order of magnitude. These ratios, in combination with the capacity for mice to metabolize a significant proportion of the BMO to BDE, are consistent with the higher susceptibility of mice than rats to BD-induced tumors. These ratios are also consistent with *in vivo* observations in which blood levels of BD epoxides and exhaled concentrations of BMO are greater in mice compared to rats after exposure to BD (16,42).

These *in vivo* metabolic constants derived from our *in vitro* studies can be incorporated into physiological models that can simulate *in vivo* behavior and the models can be used to predict blood and tissue concentrations of BD and BMO. Experiments using whole animals can then be used to verify model predictions based on *in vitro*-derived rates. Ultimately, *in vitro*-derived rates for human tissues can then be used to predict BD and BMO concentrations in human tissues as a first step in estimating risk due to BD exposure.

Acknowledgements

The authors gratefully acknowledge the assistance of Mr Max Turner in the identification of butadiene epoxides using MS and Ms Nancy Youtsey for her assistance with some of the experiments. The authors also gratefully acknowledge the numerous valuable discussions with a number of our colleagues, particularly Drs M.E.Anderson, G.L.Kedderis and M.A.Medinsky.

Appendix

The steady-state concentration of BD in the blood was calculated using the following equation taken from Andersen (44):

$$C_B^{BD} = C_{IN} Q_P \left(\frac{Q_L\, V/K}{Q_L + V/K} + \frac{Q_P}{P_B^{BD}} \right)$$

where C_B^{BD} is the steady-state blood concentration of BD (μg/l), C_{IN} is the inhaled concentration of BD (mg/l), Q_P and Q_L are alveolar ventilation and blood flow to liver (l/min), *V/K* is the rate for hepatic clearance of BD (Table VI), and P_B^{BD} is the blood/air partition coefficient for BD.

$$C_B^{BMO} = \frac{C_B^{BD}\, Q_L \left(\frac{Q_L\, V/K}{Q_L + V/K} \right) \Big/ \left(Q_L + C_T^{BMO} \right)}{(Q_P/P_B^{BMO}) + (Q_L\, C_T^{BMO}\, (Q_L + C_T^{BMO}))}$$

where C_B^{BMO} and C_B^{BD} are the steady-state blood concentrations (μg/l) of BMO and BD respectively, Q_L is blood flow to liver (l/min), *V/K* is the rate for hepatic clearance of BD to BMO (Table VI), C_T^{BMO} is the sum of all BMO clearance processes (Table VI), and P_B^{BMO} is the blood/air partition coefficient for BMO (44).

References

1. Shugaev,B B. (1969) Concentrations of hydrocarbons in tissues as a measure of toxicity. *Arch. Environ. Health*, **18**, 878–882.
2. Carpenter,C.P., Shaffer,C.B., Weil,C.S. and Smyth,H.R. (1944) Studies on the inhalation of 1,3-butadiene; with a comparison of its narcotic effect with benzol, toluol, and styrene, and a note on the elimination of styrene by the human. *J. Ind. Hyg. Toxicol.*, **26**, 69–78.
3. Brunnemann,K.D., Kagan,M.R., Cox,J.E. and Hoffmann,D. (1990) Analysis

of 1,3-butadiene and other selected gas-phase components in cigarette mainstream and sidestream smoke by gas chromatography–mass selective detection. *Carcinogenesis*, **11**, 1863–1868.
4. Pelz,N., Dempster,A.M. and Shore,P.R. (1990) Analysis of low molecular weight hydrocarbons including 1,3-butadiene as engine exhaust gases using an aluminum oxide porous-layer open-tubular fused-silica column. *J. Chromatogr. Sci.*, **28**, 230–235.
5. Environmental Protection Agency (1991) Preliminary draft list of categories and subcategories under Section 112 of the Clean Air Act. *Fed. Reg.*, **56**, 28548–28557.
6. de Meester,C., Poncelet,F., Roberfroid,M. and Mercier,M. (1980) The mutagenicity of butadiene towards *Salmonella typhimurium*. *Toxicol. Lett.*, **6**, 125–130.
7. Poncelet,F., de Meester,C., Duverger van Bogaert,M., Lambotte-Vandepaer,M., Roberfroid,M. and Mercier,M. (1980) Influence of experimental factors on the mutagenicity of vinylic monomers. *Arch. Toxicol., Suppl.*,**4**, 63–66.
8. Duverger,M., Lambotte,M., Malvoisin,E., de Meester,C., Poncelet,F. and Mercier,M. (1981) Metabolic activation and mutagenicity of 4 vinylic monomers (vinyl chloride, styrene, acrylonitrile, butadiene). *Toxicol. Eur. Res.*, **3**, 131–140.
9. Tice,R.R., Boucher,R., Luke,C.A. and Shelby,M.D. (1987) Comparative cytogenetic analysis of bone marrow damage induced in male B6C3F1 mice by multiple exposures to gaseous 1,3-butadiene. *Environ. Mutagenesis*, **9**, 235–250.
10. Cunningham,M.J., Choy,W.N., Theall,A.G., Rickard,L.B., Vlachos,D.A., Kinney,L.A. and Sarrif,A.M. (1986) *In vivo* sister chromatid exchange and micronucleus induction studies with 1,3-butadiene in B6C3F1 mice and Sprague–Dawley rats. *Mutagenesis*, **1**, 449–452.
11. Huff,J.E., Melnick,R.L., Solleveld,H.A., Haseman,J.K., Powers,M. and Miller,R.A. (1985) Multiple organ carcinogenicity of 1,3-butadiene in B6C3F1 mice after 60 weeks of inhalation exposure. *Science*, **227**, 548–549.
12. Melnick,R.L., Huff,J.E., Chou,B.J. and Miller,R.A. (1990) Carcinogenicity of 1,3-butadiene in C57BL/6 × C3H F1 mice at low exposure concentrations. *Cancer Res.*, **50**, 6592–6599.
13. Owen,P.E., Glaister,J.R., Gaunt,I.F. and Pullinger,D.H. (1987) Inhalation toxicity studies with 1,3-butadiene. III. Two year toxicity/carcinogenicity studies in rats. *Am. Ind. Hyg. Assoc. J.*, **48**, 407–413.
14. Goodrow,T., Reynolds,S., Maronpot,R. and Anderson,M. (1990) Activation of K-ras by codon 13 mutations in C57BL/6 × C3HF1 mouse tumors induced by exposure to 1,3-butadiene. *Cancer Res.*, **50**, 4818–4823.
15. Kreiling,R., Laib,R.J., Filser,J.G. and Bolt,H.M. (1986) Species differences in butadiene metabolism between mice and rats evaluated by inhalation pharmacokinetics. *Arch. Toxicol.*, **58**, 235–238.
16. Bond,J.A., Dahl,A.R., Henderson,R.F., Dutcher,J.S., Mauderly,J.L. and Birnbaum,L.S. (1986) Species differences in the disposition of inhaled butadiene. *Toxicol. Appl. Pharmacol.*, **84**, 617–627.
17. Bolt,H.M. and Filser,J.G. (1984) Inhalation pharmacokinetics based on gas uptake studies. V. Comparative pharmacokinetics of ethylene and 1,3-butadiene in rats. *Arch. Toxicol.*, **55**, 213–218.
18. Dahl,A.R., Sun,J.D., Bender,M.A., Birnbaum,L.S., Bond,J.A., Griffith,W.C., Mauderly,J.L., Muggenburg,B.A., Sabourin,P.J. and Henderson,R.F. (1991) Toxicokinetics of inhaled 1,3-butadiene in monkeys: comparison to toxicokinetics in rats and mice. *Toxicol. Appl. Pharmacol.*, **110**, 9–19.
19. Filser,J.G. and Bolt,H.M. (1984) Inhalation pharmacokinetics based on gas uptake studies. VI. Comparative evaluation of ethylene oxide and butadiene monoxide as exhaled reactive metabolites of ethylene and butadiene in rats. *Arch. Toxicol.*, **55**, 219–223.
20. Schmidt,L. and Löeser,E. (1985) Species differences in the formation of butadiene monoepoxide from 1,3-butadiene. *Arch. Toxicol.*, **57**, 222–225.
21. Kreuzer,P.E., Kessler,W., Welter,H.F., Baur,C. and Filser,J.G. (1991) Enzyme specific kinetics of 1,2-epoxybutene-3 in microsomes and cytosol from livers of mouse, rat and man. *Arch. Toxicol.*, **65**, 59–67.
22. Powis,G. and Boobies,A.R. (1975) Effect of washing of the hepatic microsomal fraction in sucrose solutions and in sucrose containing EDTA upon the metabolism of foreign compounds. *Biochem. Pharmacol.*, **24**, 1771–1776.
23. Lowry,O.H., Rosenbrough,N.F., Farr,A.L. and Randall,R.J. (1951) Protein measurement with the Folin phenol reagent. *J. Biol. Chem.*, **193**, 265–275.
24. Omura,T. and Sato,R. (1964) The carbon monoxide-binding pigment of liver microsomes. I. Evidence for its hemoprotein nature. *J. Biol. Chem.*, **239**, 2370–2378.
25. Guengerich,F.P., Kim,D-H. and Iwasaki,M. (1991) Role of human cytochrome P450 IIE1 in the oxidation of many low molecular weight cancer suspects. *Chem. Res. Toxicol.*, **4**, 168–179.
26. Peter,R., Böcker,R., Beaune,P.H., Iwasaki,M., Guengerich,F.P. and Yang,C.S. (1990) Hydroxylation of chlorzoxazone as a specific probe for human liver cytochrome P-450 IIE1. *Chem. Res. Toxicol.*, **3**, 566–573.
27. Wu,C. and Mathews,K.P. (1983) Indomethacin inhibition of glutathione S-transferase. *Biochem. Biophys. Res. Commun.*, **112**, 980–985.
28. Danielson,Y.H. and Mannervik,B. (1988) Paradoxical inhibition of rat glutathione transferase 4-4 by indomethacin explained by substrate–inhibitor–enzyme complexes in random-order sequential mechanism. *Biochem. J.*, **250**, 705–711.
29. Northrup,D.B. (1983) Fitting enzyme data to *V/K*. *Anal. Biochem.*, **132**, 457–461.
30. Kreiling,R., Laib,R.J. and Bolt,H.M. (1988) Depletion of hepatic non-protein sulfhydryl content during exposure of rats and mice to butadiene. *Toxicol. Lett.*, **41**, 209–214.
31. Malvoisin,E., Lhoest,G., Poncelet,F., Roberfroid,M. and Mercier,M. (1979) Identification and quantitation of 1,2-epoxybutene-3 as the primary metabolite of 1,3-butadiene. *J. Chromatogr.*, **178**, 419–425.
32. Bolt,H.M., Schmiedel,G., Filser,J.G., Rolzhäuser,H.P., Lieser,K., Wistuba,D. and Schurig,V. (1983) Biological activation of 1,3-butadiene to vinyl oxirane by rat liver microsomes and expiration of the reactive metabolite by exposed rats. *J. Cancer Res. Clin. Oncol.*, **106**, 112–116.
33. Elfarra,A.A., Duescher,R.J. and Pasch,C.M. (1991) Mechanisms of 1,3-butadiene oxidations to butadiene monoxide and crotonaldehyde by mouse liver microsomes and chloroepoxidase. *Arch. Biochem. Biophys.*, **286**, 244–251.
34. Malvoisin,C., Mercier,M. and Roberfroid,M. (1982) Enzymatic hydration of butadiene monoxide and its importance in the metabolism of butadiene. *Adv. Exp. Med. Biol. USA*, **136A**, 437–444.
35. Malvoisin,E. and Roberfroid,M. (1982) Hepatic microsomal metabolism of 1,3-butadiene. *Xenobiotica*, **12**, 137–144.
36. Gervasi,P.G., Citti,L., del Monte,M., Longo,V. and Benetti,D. (1985) Mutagenicity and chemical reactivity of epoxide intermediates of the isoprene metabolism and other structurally related compounds. *Mutat. Res.*, **156**, 77–82.
37. International Agency for Research on Cancer (1976) *Monographs on the Evaluation of Carcinogenic Risk of Chemicals to Man*. IARC, Lyon, Vol. 11, pp. 115.
38. Wistuba,D. (1986) Enantioselektive Metabolisierung kleiner aliphatischer Olefine und Oxirane durch cytochrom-P450-abhängige Monooxygenase, Epoxide-hydrolasen und Glutathion S-Transferasen. Eberhard-Karls Universität Tübingen.
39. Guengerich,F.P. and Shimada,T. (1991) Oxidation of toxic and carcinogenic chemicals by human cytochrome P-450 enzymes. *Chem. Res. Toxicol.*, **4**, 391–407.
40. Beaune,P., Kremers,P.G., Kamunsky,L.S., de Graeve,J. and Guengerich,F.P. (1986) Comparison of monooxygenase activities and cytochrome P-450 isozyme concentrations in human liver microsomes. *Drug. Metab. Dispos.*, **14**, 437–442.
41. Sharer,J.E., Duescher,R.J. and Elfarra,A.A. (1991) Formation, stability and rearrangements of the glutathione conjugates of butadiene monoepoxide: evidence for the formation of stable sulfurane intermediates. *Chem. Res. Toxicol.*, **4**, 430–436.
42. Kreiling,R., Laib,R.J., Filser,J.G. and Bolt,H.M. (1987) Inhalation pharmacokinetics of 1,2-epoxybutene-3 reveal species differences between rats and mice sensitive to butadiene-induced carcinogenesis. *Arch. Toxicol.*, **61**, 7–11.
43. Andersen,M.E., Clewell,H.J., III, Gargas,M.L., Smith,F.A. and Reitz,R.H. (1987) Physiologically based pharmacokinetics and the risk assessment process for methylene chloride. *Toxicol. Appl. Pharmacol.*, **87**, 185–205.
44. Andersen,M.E. (1981) A physiologically based toxicokinetic description of the metabolism of inhaled gases and vapors: analysis at steady-state. *Toxicol. Appl. Pharmacol.*, **60**, 509–526.

Received on January 14, 1992; revised on March 31, 1992; accepted on April 13, 1992